HHS Public Access

Author manuscript

Burns. Author manuscript; available in PMC 2022 December 01.

Published in final edited form as:

Burns. 2022 December ; 48(8): 1950–1965. doi:10.1016/j.burns.2022.01.012.

Evaluation of healing outcomes combining a novel polymer formulation with autologous skin cell suspension to treat deep partial and full thickness wounds in a porcine model: a pilot study

Bonnie C. Carney[a,b,h], **Mary A. Oliver**[b], **Metecan Erdi**[c], **Liam D. Kirkpatrick**[b], **Stephen P. Tranchina**[b], **Selim Rozyyev**[d], **John W. Keyloun**[b,e], **Michele S. Saruwatari**[d,e], **John L. Daristotle**[f], **Lauren T. Moffatt**[a,b,h], **Peter Kofinas**[c], **Anthony D. Sandler**[d], **Jeffrey W. Shupp**[a,b,g,h,*]

[a]Department of Biochemistry and Molecular and Cellular Biology, Georgetown University Medical Center, Washington, DC, USA

[b]Firefighters' Burn and Surgical Research Laboratory, MedStar Health Research Institute, Washington, DC, USA

[c]Department of Chemical and Biomolecular Engineering, University of Maryland, College Park, MD 20742, USA

[d]Sheikh Zayed Institute for Pediatric Surgical Innovation, Joseph E. Robert Jr. Center for Surgical Care, Children's National Medical Center, Washington, DC 20010, USA

[e]Department of Surgery, MedStar Washington Hospital Center and MedStar Georgetown University Hospital, Washington, DC, USA

[f]David H. Koch Institute for Integrative Cancer Research, Massachusetts Institute of Technology, Cambridge, MA 02139, USA

[g]The Burn Center, Department of Surgery, MedStar Washington Hospital Center, Washington, DC, USA

[h]Department of Surgery, Georgetown University School of Medicine, Washington, DC, USA

[*]Correspondence to: The Burn Center, 110 Irving Street, NW, Suite 3B-55, Washington, DC 20010, USA, jeffrey.w.shupp@medstar.net (J.W. Shupp).

CRediT authorship contribution statement

BCC, MAO, ME, LDK, SPT, and JWK performed the animal work. **ME and PK** oversaw polymer synthesis and application. **ME and JLD** performed experimentation and analysis for initial cell viability studies. **MAO** embedded, sectioned, and stained the biopsies for histology. **ME and MAO** measured percent re-epithelialization. **SR** imaged sections and analyzed data for dermal cellularity. **BCC** analyzed data and interpreted findings. **BCC** wrote the manuscript. **MSS** contributed to data analysis and manuscript preparation and editing. **LTM, PK, ADS, and JWS** reviewed and edited the manuscript, conceived of the project, acquired funding, and oversaw the research. All authors have approved of the final manuscript.

Conflicts of interest

This work was funded by AVITA Medical. M.E. was supported by the National Institute of Biomedical Imaging and Bioengineering of the National Institutes of Health under Award Number R01EB019963. JWS is a consultant for AVITA Medical. The remaining authors declare no conflicts of interest.

Appendix A. Supporting information

Supplementary data associated with this article can be found in the online version at doi:10.1016/j.burns.2022.01.012.

Abstract

Autologous skin cell suspensions (ASCS) can treat burns of varying depths with the advantage of reduced donor site wound burden. The current standard primary dressing for ASCS is a nonabsorbant, non-adherent, perforated film (control) which has limited conformability over heterogeneous wound beds and allows for run-off of the ASCS. To address these concerns, a novel spray-on polymer formulation was tested as a potential primary dressing in porcine deep partial thickness (DPT) and full thickness (FT) wounds. It was hypothesized that the polymer would perform as well as control dressing when evaluating wound healing and scarring.

DPT or FT wounds were treated with either a spray-on poly(lactic-co-glycolic acid) (PLGA) and poly(lactide-co-caprolactone) (PLCL) formulation or control ASCS dressings. Throughout the experimental time course (to day 50), we found no significant differences between polymer and control wounds in % re-epithelialization, graft-loss, epidermal or dermal thickness, or % dermal cellularity in either model. Pigmentation, erythema, elasticity, and trans-epidermal water loss (TEWL), were not significantly altered between the treatment groups, but differences between healing wounds/scars and un-injured skin were observed. No cytotoxic effect was observed in ASCS incubated with the PLGA and PLCL polymers.

These data suggest that the novel spray-on polymer is a viable option as a primary dressing, with improved ease of application and conformation to irregular wounds. Polymer formulation and application technique should be a subject of future research.

Keywords

Autologous skin cell suspension; Solution-blow spinning polymer; Wound dressings; Hypertrophic scarring; Skin grafting; Burn wound healing

1. Introduction

Excision and autografting is the standard of care for full thickness burns [1–3]. Given the significant pain and morbidity associated with donor sites, many strategies have been developed to minimize their size, including the use of meshed split thickness skin grafts (mSTSG). Despite the use of meshing, donor site wounds can be large, especially for burns involving large total body surface areas (TBSA).

The standard tools for meshing STSGs can only expand a skin graft at a ratio of 6:1. The RECELL® System is a device that allows clinicians to prepare an autologous skin cell suspension (ASCS) containing both types of epidermal-derived cells (keratinocytes and melanocytes), and dermal-derived cells (fibroblasts) using a small donor piece of autologous skin [4]. Use of this system can result in graft expansion of up to 80 times, allowing for reduced donor site burden. The applications of ASCS range from superficial donor site wounds [5], to deep partial thickness (DPT) burns [6,7] and burns with heterogeneous depths including those with full-thickness involvement. ASCS has also been used in combination with widely meshed STSG to treat deeper burns without intact dermis [8]. The benefits of using ASCS in this way was recently demonstrated in a multi-center, prospective, within-subject controlled, randomized clinical trial by Holmes et. al [8]. In a cohort of 30 patients,

comparable healing outcomes were shown between wounds treated using mSTSG alone and wounds treated with ASCS and STSG meshed using the next highest factor compared to the control. [8].

Optimal wound healing after treatment with ASCS depends heavily on the primary dressing utilized, since this dressing determines whether cells adhere to the wound bed and remain undisturbed. In addition to cellular components, non-cellular components contained within the buffer of ASCS are hypothesized to positively contribute to wound healing, and thus, keeping them contained within the wound bed is desirable. Conventional approaches for dressing ASCS, ranging from thin polymer films to alginate hydrogels, must be cut to size and can be unwieldy and time-consuming to apply, especially for large TBSA burns with surface and contour irregularity. Many have poor wound adhesive properties that involve forceful application and frequent dressing reinforcement to achieve tissue adherence. Paradoxically, the non-biodegradable adhesives and synthetic polymers that are used in commercial dressings can increase in adhesion over time and are not absorbed by the body, resulting in pain and trauma to the wound bed with dressing changes and disruption of the healing epidermis [2,4,8,9]. In order to prevent the accumulation of hematoma and exudate, care teams must regularly assess wounds by performing frequent dressing changes. This is not only a resource and time intensive process, but it can also be painful and traumatic for patients, especially pediatric patients. Additionally, despite use of sterile technique, frequent hands-on dressing changes can lead to wound infections with subsequent delays in healing which result in the development of functionally and psychologically debilitating hypertrophic scar.

The non-absorbant, non-adherent, poly ethylene terephthalate perforated film dressing that is currently supplied in the RECELL® kit was used in the two randomized control trials conducted in the United States for FDA approval [7,8]. While no formal user assessment for the dressings was present in these studies, the following information is based on the usage of this dressing by our clinical team of four independent surgeons. Positive attributes of this film dressing include its permeable, non-adherent and transparent qualities which allow for wound site monitoring without disruption of the healing process. However, it can be difficult to apply as it tends to fold itself, and often multiple sized sheets or custom cut pieces are involved to fit well within a heterogeneous wound bed. When considering the ideal wound dressing, the currently provided dressing does meet some criteria, however an alternative may be more appealing to improve ease of use. It may also potentially improve clinical outcomes.

A critical unmet need is a wound dressing that is intrinsically adhesive, easily applied, and cost-effective, while maintaining the principles of optimal wound care. Polymer fiber mats have a wide range of surgical and medical applications including tissue engineering, drug delivery, enzyme immobilization, as well as wound dressings [9]. Electrospun fibers are often seen as a candidate material, with a process that employs an electric field to produce long, ultrafine fibers. Electrospinning generally necessitates specialized high voltage equipment with electrically conductive target substrates, while also being hindered by a slow deposition rate [10]. Such limitations thereby restrict use of electrospinning for direct deposition of fiber mats in surgery. Solution blow spinning (SBS) presents a

simple airbrush apparatus, in stark contrast to an electrospinning setup, and is defined by spray deposition of a concentrated polymer solution from a volatile solvent that evaporates completely upon deposition. [10] SBS polymer fibers are similar in morphology to electrospun fibers and can be used to coat topographically diverse surfaces. Thus they can be applied to wounds of any size, depth, or shape with the advantages of sterile, hands-free application, and rapid deposition rates with improved ease of use when compared to electrospun fibers [11,12].

The use of SBS for in vivo surgical interventions is well documented, ranging from intrinsically adhesive antimicrobial burn wound dressings [13], pressure sensitive tissue adhesives [14,15], to surgical sealants for intestinal anastomosis [16,17] and hemostatic injuries [18]. Success of these materials in their respective applications is owed to either a thermally- or pressure-mediated adhesive event occurring in vivo, coupled with a distinctly fibrous morphology that facilitates absorption and reduced loss of wound exudate. In the setting of SBS burn wound dressings, these characteristics provide a continually moist wound environment to foster normal wound healing processes. This results in decreased frequency of necessary dressing changes and reduced stripping of healing epithelium in comparison to clinically adopted polyurethane controls [19,20]. This dressing, if chosen by the provider, can thus be left in place until the wound bed is re-epithelialized, after which the dressing will fall off on its own.

Selection of polymer(s) in SBS applications dictates macroscopic behavior upon deposition. The aforementioned applications of burn wound dressings, surgical sealants, and hemostatic agents all employ a basal combination of biodegradable polymers with varying molecular weights. These biodegradable and bioabsorbable polymer blends are initially deposited in a fibrous state, but then transition to a soft, conformal film. While poly(lactic-co-glycolic acid) (PLGA) and polyethylene glycol (PEG) blend materials proved to be successful in their respective success metrics, such as antimicrobial efficacy and sealant strength, large wound areas are often moist and necessitate improved wet tissue adherence without risk of stripping healthy epithelial tissue. This challenge—which is especially relevant when treating wounds with ASCS—was addressed by employing poly(lactide-co-caprolactone) (PLCL), a biodegradable elastomer that functions as a pressure sensitive adhesive (PSA) with strong wet tissue adhesion (> 1 N/cm^2) when blended at select molecular weights [14]. We have recently demonstrated that an adhesive layer of PLCL allows for complete, timely wound healing in a partial-thickness porcine wound model, with adhesive strength comparable to a commercial bandage [15].

Conventional bandages and wound dressings are coated with PSAs of varying formulations, whose mechanism of action is dependent on an ability to apply pressure to the adhesive-tissue interface without any curing event. These commercial PSAs are typically composed of non-degradable synthetic polymers and resins, and have shown to cause not only allergic contact dermatitis, but also strip a healing wound of newly deposited tissue [19]. Herein, we used tissue adhesive PLCL deposited via SBS to seal wound areas after administration of ASCS. The tacky PLCL layer also anchored a secondary layer of PLGA fibers that were deposited via SBS to ensure absorption of wound exudate, secure the dressing, and form a non-adhesive barrier to prevent unwanted adhesion or detachment of the PLCL layer.

The purpose of the current work was to investigate the ease of use, wound healing trajectory, and subsequent hypertrophic scar development when SBS polymer is used as a primary dressing over DPT and FT wounds treated with ASCS or ASCS+mSTSG. The red Duroc pig model was used in this study due to its known ability to form fibroproliferative scars in comparison with the Yorkshire pig [21–24]. It was hypothesized that wounds treated with polymer as a primary dressing would exhibit eqivalent or faster wound healing and reduced scarring due to improved adherence of the ASCS upon application.

2. Materials and methods

2.1. Preliminary cell viability assay

ASCS were isolated and diluted to a concentration of 10^6 cells/mL with the RECELL® System according to the manufacturer's specifications (AVITA Medical, Valencia, CA) using the supplied lactated ringer buffer. Solid polymer disks were prepared by depositing 10 mg of PLGA, PLCL, or blended PLGA/PEG by SBS and sterilized under ultraviolet light. Each disk was then added to 1 mL of ASCS and incubated for 1 h. The polymer disk was removed and a live/dead assay (Invitrogen, L3224) was performed on a subset of the sample. Each sample ($n = 3$ per polymer) was imaged 4 times in a different location. Images were processed using a color filter in ImageJ to identify stained live and dead cells, allowing for the quantification of the viability of the cells in the ASCS after exposure to polymer. 50% dimethyl sulfoxide was used as a positive control, and the negative control was ASCS incubated with no polymer. All results are normalized to the viability produced by the negative control.

2.2. Animal model

All animal procedures were reviewed and approved by the Institutional Animal Care and Use Committee prior to beginning the experiments, and animals were housed and cared for in compliance with all relevant regulations governing animal use in research. Details about their husbandry, enrichment, and anesthesia and monitoring have been previously published according to the ARRIVE guidelines [25]. Castrated, male, red Duroc pigs were used in this study to eliminate the potential for estrous cycling to effect wound healing [26–29].

2.3. Deep partial thickness

Two Duroc pigs (Animals 1 and 2) were used in the deep partial thickness (DPT) wounding portion of the experiment. Each animal had two wounds on each flank for a total of n = 8 total wounds for each treatment: control or polymer). On Day 0, digital images and baseline 3 mm punch biopsies of un-injured skin were taken from a site far removed from the wounding area. DPT wounds were created with a dermatome (Zimmer Biomet, Warsaw IN) set to 0.03″, and 2 passes were taken to create a 10.16 cm × 10.16 cm wound. A 2 cm × 3 cm STSG was harvested from the flank using a dermatome at a depth of 0.012″ [20] and processed using the RECELL® System to obtain ASCS (AVITA Medical, Valencia, CA). The 6 mL of prepared ASCS was split into 4, and each syringe was used to spray 1.5 mL over each DPT wound using a ratio of 1 to 80 (Video 1). A small aliquot of ASCS was collected for ASCS characterization as described below. The approximate duration between the final ASCS preparation step in the kit and wound application was 20–30 min. The

same operator prepared the ASCS in all 4 animals (as well as the preliminary cell viability assay) to attempt to reduce inter-operator variability in the makeup of ASCS cell populations that can be affected by the scraping technique unique to each operator. On half of the wound beds, the nonabsorbent, non-adherent, poly (ethylene terephthalate) perforated film (TelfaClear™ dressing, Covidien, Dublin, Ireland) was applied directly after spraying cells for the primary dressing. Herein, this will be referred to as the control dressing. The other half of the wounds were dressed with the PLCL/PLGA polymer as the primary dressing. Herein, this will be referred to as the polymer dressing. Treatment with either primary dressing was alternated in each animal due to the potential for effects of the cranial-caudal axis (Supplemental Table 1). In all wounds, the primary dressing was followed by Mepilex Ag (Molnlyke, Sweden) to provide padding. A neoprene vest was applied over the dressings to keep them in place and to protect the wound sites [21].

Supplementary material related to this article can be found online at doi:10.1016/j.burns.2022.01.012.

2.4. Full thickness

An excision, meshed split-thickness skin graft (mSTSG), ASCS model was used as previously described with modifications [25]. Two Duroc pigs (Animals 3 and 4) were used in the full thickness (FT) wounding portion of the experiment. Each animal had two wounds created on each flank for a total of n = 8 total wounds for treatment: control or polymer.

On Day 0, full thickness wounds were created with a dermatome (Zimmer Biomet, Warsaw IN) set to 0.03″, and 3 passes were taken down to subcutaneous fat to create a 10.16 cm by 10.16 cm wound. A goulian knife was used to excise excess tissue within the wound area down to the same plane. A dermatome was used to harvest STSG from the upper portion of the leg at a depth of 0.012″ [25]. A 1 cm × 6 cm portion of the STSG was saved in buffer to be used for processing into ASCS. The remainder of the STSG was meshed 4:1 (Brennan, Molnlycke) and subsequently applied to the wound beds. The donor sites were dressed with Mepilex Ag (Molnlycke).

The 6 cm^2 STSG that was not meshed was processed using the RECELL® System to obtain ASCS (AVITA Medical, Valencia) as described above in the DPT section. On half of the wound beds, the nonabsorbent, non-adherent, poly (ethylene terephthalate) perforated film dressing (TelfaClear™, Covidien) was applied directly after ASCS spray application for the primary dressing (Fig. 1A). The other half of the wounds were dressed with the polymer as the primary dressing. In all wounds, Xeroform™ dressing was the secondary dressing (Medtronic, Minneapolis, MN) (Fig. 1B). Finally, a tie-over bolster dressing (Dukal Corporation, Ronkonkoma, NY) was constructed as the final component of the dressing (Fig. 1C). Application of the vests were the same as for DPT wounds.

2.5. Polymer formulations and solution blowspinning process

Both 100 mg/mL PLGA (Mn = 48,800 ± 450 Da, 50:50 L:G, $15/g, $18/wound, Lactel) and 200 mg/mL PLCL (Mn = 35,000–45,000 Da, 70:30 L:CL, acid endcap, $18/g, $11/wound, Akina) compositions were dissolved in ethyl acetate and loaded into a portable airbrush (0.2 mm nozzle, G22, Master Airbrush) attached to either 16 g CO_2 cartridges (Cycling

Deal) for DPT wounds or an air compressor (Temptu) for FT wounds with regulators set at pressures of 20 psi on both instruments. 5–6 mL of tissue adhesive PLCL was initially spray-deposited following administration of ASCS as to ensure full wound coverage. This initial dressing was followed by spray deposition of 5–6 mL of non-adhesive PLGA dressing to create a dual-polymer layer material. An example of the polymer application process for DPT wounds is shown in Video 3 and for FT wounds in Video 4.

Supplementary material related to this article can be found online at doi:10.1016/j.burns.2022.01.012.

2.6. Experimental time course for all wounds

For both wound depths, on postoperative Day 3, all secondary dressings were removed, leaving the control or polymer dressings in place. For the full thickness wounds, most of the polymer was removed as it stuck to the Xeroform. As such, the polymer was re-applied after sample acquisition to mimic the control timeline of application (this was not necessary for the DPT wounds). For DPT wounds, 3 mm punch biopsies were taken of the wound sites. For FT wounds, 3 mm punch biopsies were taken of the autografted sites (from specific areas of mSTSG and interstices were taken through the dressings) and of the donor sites. Following the acquisition of samples, the secondary dressings were replaced, Mepilex Ag was added for additional padding, and a neoprene vest was secured around the animal. The donor sites were dressed as described above for Day 0.

On Day 5, a wound assessment took place. All dressings were removed carefully. Digital pictures were taken of the autografted sites percent re-epithelialization assessments. For FT wounds, graft-take was assessed using a subjective scale [22]. Punch biopsies for DPT and FT wounds were taken as above. The wounds were re-dressed as described above.

On Days 7, 9, and 12, a wound assessment took place as described above. Punch biopsies were taken as described above. Additionally, non-invasive skin probes were used to measure erythema, melanin, elasticity, and TEWL (Delfin Technologies, Stamford, CT). On Days 22, 29, 36, 43, and 50, a scar assessment took place, similar to the wound assessments above.

2.7. ASCS characterization

Cell counts and percent viability were assessed using standard trypan blue dye techniques. Invitrogen™ Molecular Probes™ LIVE/DEAD™ Viability/Cytotoxicity Kit, for Mammalian Cells (Invitrogen, L3224) was used according to the manufacturer's protocol as previously described [25]. Eight fields of view were imaged. This process was repeated for each cell suspension.

2.8. Re-epithelialization

Digital pictures were used to measure percent re-epithelialization using ImageJ software (NIH, Bethesda, MD).

2.9. Graft loss grading scale

For the FT wounds, graft-loss was assessed by two independent blinded assessors on Day 5 after the primary dressings were removed as previously described [25,30]. The questionnaire consists of the following questions, and a grade was assigned at the end based on Supplemental Table 2. Average scores based on both assessors were calculated.

1. Is there any graft loss?
2. If yes, assign percentage
3. If yes, assign likely cause (shear, infection)
4. Assign Grade

2.10. Histology

2.10.1. Sample processing—Punch biopsies which were previously formalin-fixed were embedded in paraffin (FFPE) and sectioned at 6 μm on glass slides. Sections were stained with H&E and imaged under bright field microscopy.

2.10.2. Epidermal and dermal thickness—H&E-stained sections were imaged at 5X. Epidermal and dermal thickness were measured for the DPT wounds on Days 5, 9, and 12. For the FT wounds, Days 3, 7, and 12 were used. In these biopsies from FT wounds, one was taken from an area within the interstice, while one biopsy was taken from an area that had adhered mSTSG. Data was collected for each of these sample types separately. One section per animal per time point was viewed, and 3 measurements were taken per section. Measurements were carried out using Image J.

2.10.3. Dermal cellularity—H&E-stained sections were imaged at 40X. Dermal cellularity was measured at the same timepoints as described above for epidermal and dermal thickness. One section per animal per time point was viewed, and 3 distinct high-powered fields of view were taken per section. Within ImageJ, the images were converted to an RGB stack. A threshold of 149 was set, and the % area of the image stained purple by hematoxylin was obtained for each image.

2.10.4. Statistical analysis—Relative cell viability between different polymer formulations was compared using a one-way ANOVA with Tukey's correction for multiple comparisons. In both DPT and FT wounds, percent re-epithelialization between polymer vs. control groups was compared using a two-way ANOVA with Sidak's correction for multiple comparison at each timepoint after injury. In both DPT and FT wounds, elasticity, TEWL, erythema, and melanin were compared between polymer, control, and un-injured skin using a two-way ANOVA with Tukey's correction for multiple corrections at each timepoint after injury. In both DPT and FT wounds, epidermal and dermal thickness were compared between polymer and control groups using a two-way ANOVA with Sidak's correction for multiple comparisons at each timepoint after injury. This was a pilot study, and therefore, a power analysis was not calculated to determine the number of wounds or scars that would have been necessary to achieve 80% power to reject the null hypothesis.

3. Results

3.1. PLGA and PLCL polymers do not negatively affect ASCS viability

ASCS are sensitive to processing conditions and certain compounds [14]. To assess the compatibility of various tissue adhesive polymers that have previously been used as wound dressings [4,13], the ASCS were processed in the presence of polymer disks and then the relative viability of the resulting ASCS was assessed (Fig. 2). Due to the high proportion of water-soluble low molecular weight PEG necessary for effective adhesion, PLGA/PEG had a significantly negative effect on relative cell viability. However, the two biodegradable, structural polymers tested, PLGA and PLCL, had no effect on relative cell viability. We hypothesized that a combination of PLGA and PLCL could be used to create an adhesive wound dressing, given the inherent tissue adhesion supplied by elastomeric PLCL and the high strength of fiber-forming PLGA.

3.2. The wound healing trajectory in deep partial thickness wounds that were sprayed with ASCS is not negatively impacted by application of polymer as a primary dressing

3.2.1. Autologous skin cell suspension characterization—Trypan blue staining revealed that the ASCS was ~45% viable, and a total of 8.9–9.55E5 cells/cm^2 were sprayed onto the DPT wounds (Supplemental Fig. 1, Supplemental Table 3). Fluorescent staining revealed that the ASCS was ~40% viable, and a total of 7.88E5–1.31E6 cells/cm^2 were sprayed onto the DPT wounds.

3.2.2. Gross images of healing wounds—In Animal 1, the most cranial wound that was treated with polymer had a hematoma formation under the polymer that can be seen in the images through Day 9. Despite this formation which caused the wounds to look largely different from each other through Day 9, the wounds healed in a similar manner, and were 100% re-epithelialized by Day 12 based on images (Fig. 3A). By Days 44 and 50, some degree of hypertrophy can be visualized, although this is not different based on primary dressing treatment. In Animal 1, the caudal wounds healed similarly to each other, and to the cranial wounds (Supplemental Fig. 2).

In Animal 2, the most cranial wounds healed similar to each other despite primary dressing application (Supplemental Fig. 3). This animal was also 100% re-epithelialized by Day 12. Beginning at Day 29 and through Day 49, large areas of hypertrophy can be visualized that progress to be hyper-pigmented versus normal skin. This hypertrophy occurred regardless of primary dressing, but displayed a greater degree of hypertrophy compared to Animal 1. The caudal wounds in Animal 2 were similar to the cranial wounds (Supplemental Fig. 4).

3.2.3. Re-epithelialization—The percent re-epithelialization between control vs. polymer groups was not different at any time point (Fig. 3B). At Day 5, re-epithelialization percentages were 68.84 ± 9.8% vs. 70.49 ± 8.4% in control vs. polymer groups. Wounds progressed to ~80% re-epithelialized at Day 7% and 90% at Day 9 irrespective of primary dressing type. Wounds were 100% re-epithelialized by Day 12.

3.3. Non-invasive skin probes

3.3.1. Pigmentation and erythema are not altered by DPT wound treatment with control or polymer as primary dressing over ASCS—Erythema was not different between control vs. polymer groups at any time point (Fig. 4A). Erythema decreased over time. ASCS-treated DPT wounds resulted were statistically significant hypo-pigmented at Days 9 and 12 (Uninjured=890.42 ± 21.05 vs. control=808.83 ± 18.17 and polymer=765.50 ± 23.03, n = 4, $p < 0.01$, Day 9). Melanin index in the DPT healing wounds vs. un-injured stabilized at Day 22, and remained constant throughout the time-course through Day 50. Although hypopigmentation was observed between the DPT wounds and uninjured skin, this was not dependent on primary dressing type (Fig. 4).

3.3.2. Elasticity and TEWL are not altered by DPT wound treatment with control or polymer as primary dressing over ASCS—We found no significant differences in elasticity between control vs. polymer groups at any time point (Fig. 4C). Stiffness decreased over time in the DPT wounds, and hence, elasticity improved. Overall, we found few differences in TEWL at any of the time points. At Day 29, scars resulting from polymer-treated wounds had increased TEWL compared to un-injured skin ($p < 0.05$). At Day 36, un-injured skin had increased TEWL compared to both treatment groups (Fig. 4D).

3.4. Histological data

3.4.1. Architecture—Representative H&E staining of DPT wounds are shown (control vs. polymer: Fig. 5, Supplemental Fig. 5). We found some appreciable differences in histomorphometric structure between groups. The control tissues contained more adnexal structures that in the polymer groups. In addition, a trend towards increased inflammatory cell infiltrate was present in the polymer treated wounds at Days 5 and 9.

In both groups, at Day 5, neo-epidermal formation can be viewed with a surrounding area of inflammatory cell infiltrate. The remaining reticular dermis contained a % cellularity that was normal compared to un-injured skin. We found some instances of epidermal pockets that may suggest that ASCS cells attached and proliferated in those areas. Skin structures such as glands and hair follicles are present. At Day 9, a thickening and stratification of the epidermis can be observed. We found dramatically increased dermal cellularity that is demarcated by the normal dermis underneath, presumably from the un-injured skin that remained after wounding. Once again, dermal appendages are prevalent. At day 12, a thicker layer of increased dermal cellularity was found with some epidermal structural maturation with rete ridge formation.

3.4.2. Epidermal and dermal thickness—We found no significant differences in the epidermal or dermal thickness between control vs. polymer groups at any time point (Fig. 6A and 6B). At Day 5, the epidermal thickness was 78.94 ± 18.09 vs. 87.34 ± 16.99 μm and the dermal thickness was 1458.52 ± 189.29 vs. 1108.153 ± 225.69 μm in control and polymer groups, respectively. Dermal thickness increased throughout the time course from ~1000 μm at Day 5 to ~1500 μm at Day 9 and 12. Epidermal thickness remained constant over time.

3.4.3. Cellularity—Dermal cellularity was not different between control vs. polymer groups at any time point (Fig. 6C). At Day 5, the dermal cellularity was 4.25 ± 1.36 vs. 3.125 ± 0.679 vs. 3.432 ± 0.421% in control, polymer, and un-injured skin groups respectively.

3.5. The wound healing trajectory in FT wounds that were autografted with mSTSG and sprayed with ASCS is not negatively impacted by application of polymer as a primary dressing

3.5.1. Autologous skin cell suspension characterization—Trypan blue staining revealed that the ASCS was ~77% viable, and a total of 7.65–8.4E5 cells/cm^2 were sprayed onto the FT wounds (Supplemental Fig. 6, Supplemental Table 4). Fluorescent staining revealed that the ASCS was ~55% viable, and a total of 1.20E5–1.42E6 cells/cm^2 were sprayed onto the FT wounds.

3.5.2. Gross images of healing wounds—In Animal 3, the most cranial wounds healed similar to one another. We found near 100% graft adherence with no loss noted in either group (Fig. 7A). These wounds were 100% re-epithelialized by Day 9. At Day 22 in the polymer-treated wound, some hyper-pigmentation can be observed due to post-inflammatory hyper-pigmentation from a biopsy punch taken at the previous timepoint that persisted through Day 50. This is most likely due to animal interference by itching or otherwise interfering with the healing at that timepoint.

In Animal 3, in the most caudal wound that was treated with control dressing, a small amount of graft-loss was present along the seam of the graft most likely due to shear forces which moved the graft. The contralateral wound that was treated with polymer did not have this graft loss (Supplemental Fig. 7). This graft-loss, in the otherwise well-adhered graft, caused an open wound area through Day 9. Despite these differences, the wounds with different primary dressing healed very similarly and were re-epithelialized by Day 12.

In Animal 4, the most cranial wound that was treated with control had similar graft slippage as mentioned above. This slippage led to open wound area through Day 9, but otherwise, the wounds healed and were re-epithelialized by Day 12 (Supplemental Fig. 8). The most caudal wounds likewise healed similarly (Supplemental Fig. 9). All donor site wounds were re-epithelialized by Day 14. All wounds healed with minimal characteristics of hypertrophic scar at Day 49 and were visually similar to surrounding un-injured skin, albeit without hair follicles.

3.5.3. Re-epithelialization—The percent re-epithelialization was not significantly different between control vs. polymer groups at any time point (Fig. 7B). At Day 5, re-epithelialization percentages were 46.37 ± 3.28% vs. 42.40 ± 2.15% in control vs. polymer groups. Wounds progressed to ~85% re-epithelialized at Day 7. Wounds were 100% re-epithelialized by Day 9.

3.5.4. Graft-loss grading scale—Graft-loss was only assessed at Day 5 when the primary dressings were removed for the first time. Graft-loss was small in the wounds as graded by blinded assessors. In Animal 3, the most caudal wound on the right flank (which

was treated with control dressing) was given a Grade II (Table 1). Both of the wounds on the left flank were given scores of I, indicating minimal graft loss. In Animal 4, a range of scores were given. Overall, at Day 5 the polymer group had a score of 0.88 ± 0.31 vs. 1.4 ± 0.38 in the control group, indicating increased, but non-significant graft-loss in the control group.

3.6. Non-invasive skin probes

3.6.1. Pigmentation and erythema are altered by FT wound treatment with control or polymer as primary dressing over ASCS—Erythema was not different between control vs. polymer groups at any time point (Fig. 8A). Erythema was significantly increased in un-injured skin at all timepoints. Overall, ASCS-treated FT wounds resulted in hypo-pigmentation observed at Days 9, 12, and 22 (Uninjured= 834.08 ± 8.12 vs. control=724.33 ± 21.84 and polymer=739.33 ± 22.10, $n = 4$, $p < 0.01$, Day 9). Melanin index in the FT healing wounds vs. un-injured evened out at Day 29, and remained constant throughout the time-course through Day 50. Although differences between the FT wounds and uninjured skin was found, this was not dependent on primary dressing group (Fig. 8B).

3.6.2. Elasticity and TEWL are not altered by FT wound treatment with control or polymer as primary dressing over ASCS—We found minimal differences in elasticity between control vs. polymer groups at any time point (Fig. 8C). At Days 36 and 43, stiffness was significantly elevated in the polymer and control groups compared to un-injured skin, respectively. Overall, few differences in TEWL were detected at any of the time points (Fig. 8D). At Day 9, un-injured skin had increased TEWL compared to treated groups ($p < 0.01$). At Day 22, the same finding was observed.

3.7. Histological data

3.7.1. Architecture—Representative H&E staining of FT wounds are shown from biopsies originating from the wound interstice (control vs. polymer, interstice biopsies: Fig. 9 and Supplemental Fig. 10). Representative H&E staining of FT wounds are shown from biopsies originating from areas of the wound that had adhered graft (control vs. polymer, mSTSG biopsies: Fig. 10 and Supplemental Fig. 11). We found no appreciable differences in histomorphometric structure of FT wounds between primary dressing treatment groups.

For the biopsies that were taken of the interstices, for both groups, at Day 3, dermal tissue was scant, and the majority of the section is subcutaneous fat. At Day 7, hyper-cellularity was found compared to un-injured skin throughout the thickness of the biopsy and thick epidermis formation. By Day 12, some hyper-cellularity is resolved, and the epidermis becomes more similar to un-injured skin. No dermal appendages were observed in any sections.

For the biopsies that were taken of the mSTSG areas, for both groups, at Day 3, epidermis was intact and a split thickness dermis engrafted over a bed of subcutaneous tissue. By Day 7, the dermis is thickened and contains some inflammatory cell infiltrate. The epidermis has a large number of rete ridges. By Day 12, some inflammatory cell infiltrate has resolved, and the epidermis looks more similar to un-injured skin.

3.7.2. Epidermal and dermal thickness—Neither epidermal or dermal thickness were different between control vs. polymer groups at any time point in the biopsies obtained from the mSTSG (Fig. 11A and 11B) or the interstice (Fig. 11D and 11E). At Day 3, the epidermal thickness was 32.10 ± 11.92 vs. 52.94 ± 7.95 μm and the dermal thickness was 329.79 ± 58.31 vs. 597.92 ± 146.47 μm in control and polymer groups respectively in the mSTSG samples. Dermal thickness increased throughout the time course from ~100 μm at Day 3 to ~1000 μm at Days 7 at Day 12 in both groups. Epidermal thickness remained relatively constant over time in both groups.

3.7.3. Cellularity—Dermal cellularity was not different between control vs. polymer groups at any time point. In both groups, cellular infiltrate was increased compared to un-injured skin in both groups at Days 7 and 12 ($p < 0.001$) (Fig. 11C and 11F). At Day 7, the dermal cellularity was 9.25 ± 3.56 vs. 8.92 ± 3.17 vs. 2.14 ± 0.61% in control, polymer, and un-injured skin groups respectively for the mSTSG group.

4. Discussion

4.1. Summary

The purpose of this study was to investigate a novel polymer formulation as a potential primary dressing for wounds treated with ASCS. It was hypothesized that treatment with polymer would not be cytotoxic to cells, and hence, wounds treated with polymer would heal similarly to wounds treated with the current standard, manufacturer-supplied, control dressing as the primary dressing.

Two different wounds types were used in this experiment: DPT and FT. In this experiment, wound re-epithelialization was used to evaluate the hypothesis. Gross images of healing wounds, direct quantitative measurements of percent re-epithelialization, and quantitative evaluations of graft-loss indicated no difference in healing outcomes between primary dressing treatment groups. All wounds were fully re-epithelialized by Day 12. This healing timecourse is within the limits of what is known in the literature to result in a lower chance for hypertrophic scar development [23–26]. Therefore, regardless of primary dressing application, these wounds closed within two weeks and had minimal scar pathology. The incorporation of these longer term scarring outcome metrics dicated the use of the red Duroc pig in this study due to its known tendency to form hypertrophic scars that are similar to human hypertrophic scars and are more severe than scars that develop in Yorkshire white pigs [21].

4.2. Usage of polymer as a primary dressing

While the supplied, control is a functional dressing, its usability in the context of ASCS delivery to wound beds could be improved upon. One disadvantage of using this control dressing is that it is permeable, and non-adherent with no seal created to keep the sprayed cells in place. The polymer, on the other hand created a sealed wound bed that limits cell or non-cellular components of the buffer from leaking out. The polymer was easily applied through a touch-free spray-nozzle, and it adhered well to the ASCS-coated wound bed that

had been sprayed with ASCS. Tearing or breaking of the polymer layer was not an issue. The polymer was flexible, and conformed to the size and shape of the wound bed.

The application of polymer was prolonged compared to control dressing application. For both wound types, the average time for application was ~15 min per wound. Two different layers of polymer were applied: one that was sticky that adhered to the wound bed, and a non-adherent outer layer. Each polymer had 5–6 mL sprayed onto each wound bed. The timing associated with spraying polymer can be optimized in future work by adjusting the volume of polymer sprayed, and working with a more industrialized setup that would allow for more efficient spraying. The initial polymer deposition was applied slowly at a safe distance to avoid blowing the cells or buffer off the wound bed. After the first layer was applied, higher pressure and faster application was possible. In this experiment, a volume that was higher than what was used in past modeling with superficial partial thickness (SPT) injuries in porcine species was chosen. A higher volume was chosen in an attempt to control for the fact that these DPT and FT would be more exudative compared to SPT wounds treated with polymer in the past. It is possible that only half of the polymer solution volume, or even less, may efficiently seal a wound bed, and thus the duration of application can be shortened when coupled with a faster flowrate from airbrush setup. Such a contrast in deposition rate and wound sealing was noted in both wound models, where DPT wounds employed multiple CO_2 cannisters in order to spray entire polymer solution volume, and FT wounds used a compressed air setup that deposited PLCL and PLGA solutions in rapid fashion. For both DPT and FT wounds, molecular weight blends of PLCL that optimize tissue adhesive strength and material cohesive strength in published work on SPT porcine wound models draw significant interest as an improved wound dressing material.

4.3. Gross evaluation

The polymer behaved differently than expected when used on DPT wounds compared to the SPT wounds tested previously. In the instance of SPT wounds, the polymer remained as a single sheet that didn’t break or tear throughout the time period after injury. For the DPT wounds, at Day 3, when the outer dressing was taken down, it was clear that the polymer did not remain as one single unit sheet. Although this makes for a somewhat unconventional looking wound bed, the polymer did not have a cytotoxic effect on the ASCS as determined by healing outcomes. On FT wounds, Xeroform was applied as a secondary dressing cover to both the control and the polymer wounds. When the Xeroform was taken off, the entire polymer sheet came off with it. This adherence to secondary dressings is a point of future research. If a different dressing had been used, the polymer may have stayed intact on the wound bed and a second application not indicated. Furthermore, it is entirely possible that no outer dressing is needed and that the polymer dressing alone would suffice for wound care, especially in a controlled environment in the clinical setting. Also if areas of the polymer crack or detach, it is simple to blow more polymer at any time point without touching or handling the actual wound or wound bed.

4.4. Percent Re-epithelialization evaluation

We found no differences in percent re-epithelialization between the control vs. polymer groups in the DPT or the FT wounds. However, some differences were found between the

different animals as is evidenced by the standard deviations and the differences in gross healing outcomes among animals. This difference could be due to the fact that different cell populations were isolated when preparing the ASCS. It has been reported in prior literature that ASCS contains ~65% keratinocytes, 30% fibroblasts, and 3.5% melanocytes [4]. These analyses were reported from excised skin from elective abdominoplasty surgery and no reports on whether multiple patients were used to determine the percentages of cells. It is possible that the standard deviations reported are derived from a single patient tissue that had multiple different pieces of skin graft taken and multiple ASCSs prepared. It is also possible, that the data is derived from multiple donors. Hence, in future experiments evaluating re-epithelialization, ASCS makeup should be characterized using flow cytometry to ensure that the cell populations used to treat different experimental groups are equivalent. This is specifically important in porcine studies where ASCS cell population percentages have not yet been characterized. In this experiment, experimental group (polymer vs. control) were equally split among each animal, and therefore, the number of wounds in each group that received differing ASCS preparations was the same. Therefore, it is unlikely that differences in cell populations could have contributed to any minimal differences observed among polymer vs. control groups, but it possible that it contributed to differences in healing among animals.

4.5. Non-invasive skin probe evaluation

Unsurprisingly, we saw no differences between the control vs. polymer groups at any of the timepoints for erythema, melanin, elasticity, or TEWL. For melanin, in both the DPT and FT wounds, the wounds were hypo-pigmented compared to normal skin early on during the time course, and returned to normal pigmentation comparable to un-injured areas within a month of injury. For erythema, in the DPT was generally downwards until Day 29, whereafter the erythema was increased. In observing the gross images for the DPT wounds, the Day 36 timepoint is where extensive hyperpigmented dyschromia was observed in one of the animals. This dyschromia likely masked the ability of the erythema probe to accurately detect redness. This data adds to the body of knowledge that surrounds the pros and cons of non-invasive probes for measuring scar properties. In general, elasticity, or stiffness, was high at Day 9, and trended down over time through Day 50 in the DPT wounds. This data suggests that scars were getting better over time, which is the known trajectory for hypertrophic scars. TEWL showed some dynamic changes, wherein, at one timepoint, the scars had higher TEWL, and at another timepoint, the un-injured skin had higher TEWL. This data highlights how changes to the animal housing environment or surgical skin prep method may have an effect on un-injured skin TEWL. The FT, grafted wounds healed very well, and most non-invasive parameters showed that these healed wounds were very similar to normal, un-injured skin in their pigmentation, pliability, and TEWL.

4.6. Histological evaluation

The histological data agreed with the pictures and non-invasive skin probes, and showed no differences between control or polymer groups. In DPT wounds, neo-epidermis was visualized as early as Day 7 after wounding, and by Day 12, the wound bed was fully re-epithelized. In the FT wounds, biopsies were taken of the areas of mSTSG and the areas of interstices within those grafts. These replicate biopsies showed differential healing of

each area of the grafted wound, and show the heterogeneity of the healing. All wounds showed a degree of histologic re-epithelization by Day 7.

4.7. Future studies

Future work can be aimed at optimizing polymer application to shorten timing, increase efficiency, and improve wound re-epithelialization and reduce scarring. It is difficult to interpret findings without a negative control group that did not receive ASCS application. It is unclear if a difference would be found in healing potential between ASCS and non-ASCS groups based on the metrics that we used in this experiment (% re-epithelialization, non-invasive skin probes, and histological characterization). Therefore, it is difficult to tell if the polymer application helped to seal the cells in place and contributed to the advanced healing that may occur with ASCS application. These negative controls should be incorporated into future experiments. In addition, fluorescent cell labeling of ASCS should be considered to visualize cells throughout the time courses.

One limitation of this study is the low number of wounds/scars that were evaluated. Particularly in the DPT model, large standard deviations were reported for some of the outcome variables. Therefore, in future work, to reject the null hypothesis of no difference in outcome variables, a larger number of wounds would need to be included. When choosing percent re-epithelialization at Day 5 as the primary outcome for the study, based on this pilot data, group sample sizes of 26 wounds for each condition (104 total for 4 groups) would be required to achieve 80% power to reject the null hypothesis of equal means when the clinically meaningful difference in re-epithelialization is 10% with a standard deviation for both groups of 10% and with a significance level (alpha) of 0.01 (after Sidak's multiplicity correction) using a two-sided two-sample equal-variance t-test in the post-hoc Sidak's multiple comparisons tests.

5. Conclusions

Based on pilot data, the use of PLCL/PLGA polymer as a primary dressing is not cytotoxic to cells and does not impair wound healing. As determined by digital pictures, % re-epithelialization, and grading of graft-loss, healing was the same between the polymer and control groups with all wounds healing by 12 days. Blow spun polymer is possibly a novel, bio-degradable and efficient primary or secondary wound dressing for partial or full-thickness burn injuries. In the future, ASCS and polymer application should occur via the same device to simultaneously and efficiently deposit the complete wound dressing.

Supplementary Material

Refer to Web version on PubMed Central for supplementary material.

Abbreviations:

ASCS	autologous skin cell suspensions
DPT	deep partial thickness

FFPE	formalin-fixed paraffin embedded
FT	full thickness
mSTSG	meshed split thickness skin graft
PEG	poly(ethylene glycol)
PLCL	poly(lactide-co-caprolactone)
PLGA	poly(lactic-co-glycolic acid)
PSA	pressure sensitive adhesive
SBS	solution blow spinning
TBSA	total body surface area
TEWL	trans-epidermal water loss

references

[1]. Caldwell FT Jr., Wallace BH, Cone JB. Sequential excision and grafting of the burn injuries of 1507 patients treated between 1967 and 1986: end results and the determinants of death. J Burn Care Rehabil 1996;17:137–46. 10.1097/00004630-199603000-00007 [PubMed: 8675503]

[2]. Gacto-Sanchez P Surgical treatment and management of the severely burn patient: review and update. Med Intensiv 2017;41:356–64. 10.1016/j.medin.2017.02.008

[3]. Israel JS, Greenhalgh DG, Gibson AL. Variations in burn excision and grafting: a survey of the american burn association. J Burn care Res: Publ Am Burn Assoc 2017;38:e125–32. 10.1097/BCR.0000000000000475

[4]. Wood FM, Giles N, Stevenson A, Rea S, Fear M. Characterisation of the cell suspension harvested from the dermal epidermal junction using a ReCell(R) kit. Burn: J Int Soc Burn Inj 2012;38:44–51. 10.1016/j.burns.2011.03.001

[5]. Hu Z, et al. Randomized clinical trial of autologous skin cell suspension for accelerating re-epithelialization of split-thickness donor sites. Br J Surg 2017;104:836–42. 10.1002/bjs.10508 [PubMed: 28379607]

[6]. Gravante G, et al. A randomized trial comparing ReCell system of epidermal cells delivery versus classic skin grafts for the treatment of deep partial thickness burns. Burn: J Int Soc Burn Inj 2007;33:966–72. 10.1016/j.burns.2007.04.011

[7]. Holmes Iv JH, et al. A comparative study of the ReCell(R) device and autologous spit-thickness meshed skin graft in the treatment of acute burn injuries. J Burn care Res: Publ Am Burn Assoc 2018;39:694–702. 10.1093/jbcr/iry029

[8]. Holmes JH t, et al. Demonstration of the safety and effectiveness of the RECELL((R)) system combined with split-thickness meshed autografts for the reduction of donor skin to treat mixed-depth burn injuries. Burn: J Int Soc Burn Inj 2019;45:772–82. 10.1016/j.burns.2018.11.002

[9]. Xue J, Wu T, Dai Y, Xia Y. Electrospinning and electrospun nanofibers: methods, materials, and applications. Chem Rev 2019;119:5298–415. 10.1021/acs.chemrev.8b00593 [PubMed: 30916938]

[10]. Daristotle JL, Behrens AM, Sandler AD, Kofinas P. A review of the fundamental principles and applications of solution blow spinning. ACS Appl Mater Interfaces 2016;8:34951–63. 10.1021/acsami.6b12994 [PubMed: 27966857]

[11]. Katti DS, Robinson KW, Ko FK, Laurencin CT. Bioresorbable nanofiber-based systems for wound healing and drug delivery: optimization of fabrication parameters. J Biomed Mater Res B Appl Biomater 2004;70:286–96. 10.1002/jbm.b.30041 [PubMed: 15264311]

[12]. Payam Zahedi IR, Ranaei-Siadat Seyed-Omid, Jafari Seyed-Hassan, Supaphol Pitt. A review on wound dressings with an emphasis on electrospun nanofibrous polymeric bandages. Polym Adv Technol 2010. 10.1002/pat.1625

[13]. Daristotle JL, et al. Sprayable and biodegradable, intrinsically adhesive wound dressing with antimicrobial properties. Bioeng Transl Med 2020;5:e1014910.1002/btm2.10149

[14]. Daristotle JL, et al. Pressure-sensitive tissue adhesion and biodegradation of viscoelastic polymer blends. ACS Appl Mater Interfaces 2020;12:16050–7. 10.1021/acsami.0c00497 [PubMed: 32191429]

[15]. Daristotle JL, et al. Biodegradable, tissue adhesive polyester blends for safe, complete wound healing. ACS Biomater Sci Eng 2021. 10.1021/acsbiomaterials.1c00865

[16]. Behrens AM, et al. In situ deposition of PLGA nanofibers via solution blow spinning. ACS Macro Lett 2014;3:249–54. 10.1021/mz500049x [PubMed: 35590515]

[17]. Kern NG, et al. Solution blow spun polymer: a novel preclinical surgical sealant for bowel anastomoses. J Pedia Surg 2017;52:1308–12. 10.1016/j.jpedsurg.2016.11.044

[18]. Daristotle JL, et al. Improving the adhesion, flexibility, and hemostatic efficacy of a sprayable polymer blend surgical sealant by incorporating silica particles. Acta Biomater 2019;90:205–16. 10.1016/j.actbio.2019.04.015 [PubMed: 30954624]

[19]. Widman TJ, Oostman H, Storrs FJ. Allergic contact dermatitis from medical adhesive bandages in patients who report having a reaction to medical bandages. Dermatitis 2008;19:32–7. [PubMed: 18346394]

[20]. King A, Stellar JJ, Blevins A, Shah KN. Dressings and products in pediatric wound care. Adv Wound Care (N Rochelle) 2014;3:324–34. 10.1089/wound.2013.0477

[21]. Zhu KQ, Carrougher GJ, Gibran NS, Isik FF, Engrav LH. Review of the female Duroc/Yorkshire pig model of human fibroproliferative scarring. Wound Repair Regen: Publ Wound Heal Soc Eur Tissue Repair Soc 2007;15(Suppl 1):S32–9. 10.1111/j.1524-475X.2007.00223.x

[22]. Harunari N, et al. Histology of the thick scar on the female, red Duroc pig: final similarities to human hypertrophic scar. Burn: J Int Soc Burn Inj 2006;32:669–77. 10.1016/j.burns.2006.03.015

[23]. Carney BC, et al. Pigmentation diathesis of hypertrophic scar: an examination of known signaling pathways to elucidate the molecular pathophysiology of injury-related dyschromia. J Burn care Res: Publ Am Burn Assoc 2018. 10.1093/jbcr/iry045

[24]. Carney BC, et al. Reactive oxygen species scavenging potential contributes to hypertrophic scar formation. J Surg Res 2019;244:312–23. 10.1016/j.jss.2019.06.006 [PubMed: 31302330]

[25]. Carney BC, et al. A pilot study of negative pressure therapy with autologous skin cell suspensions in a porcine model. J Surg Res 2021;267:182–96. 10.1016/j.jss.2021.05.010 [PubMed: 34153561]

[26]. Ashcroft GS, Mills SJ. Androgen receptor-mediated inhibition of cutaneous wound healing. J Clin Investig 2002;110:615–24. 10.1172/JCI15704 [PubMed: 12208862]

[27]. Ashcroft GS, et al. Estrogen accelerates cutaneous wound healing associated with an increase in TGF-beta1 levels. Nat Med 1997;3:1209–15. 10.1038/nm1197-1209 [PubMed: 9359694]

[28]. Gilliver SC, Ashworth JJ, Ashcroft GS. The hormonal regulation of cutaneous wound healing. Clin Dermatol 2007;25:56–62. 10.1016/j.clindermatol.2006.09.012 [PubMed: 17276202]

[29]. Jorgensen LN, Sorensen LT, Kallehave F, Vange J, Gottrup F. Premenopausal women deposit more collagen than men during healing of an experimental wound. Surgery 2002;131:338–43. 10.1067/msy.2002.119986 [PubMed: 11894040]

[30]. Nosanov LB, et al. Graft loss: review of a single burn center's experience and proposal of a graft loss grading scale. J Surg Res 2017;216:185–90. 10.1016/j.jss.2017.05.004 [PubMed: 28807206]

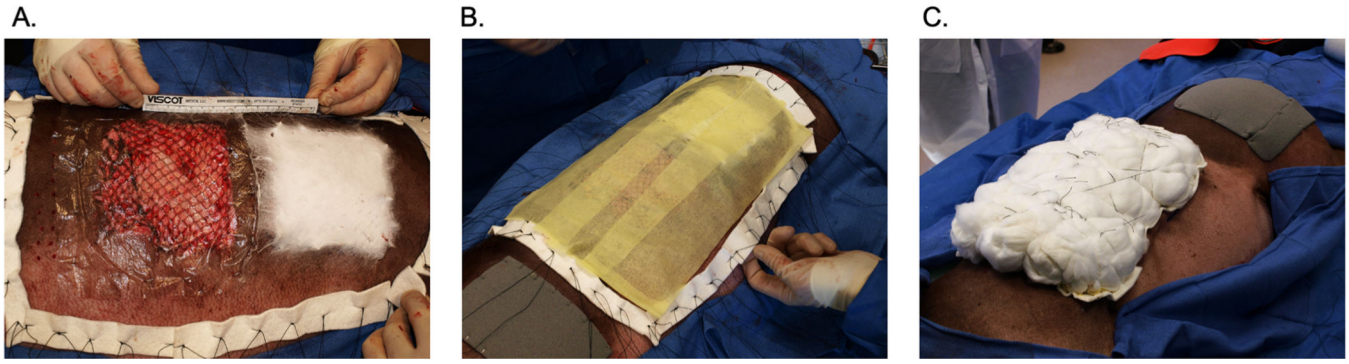

Fig. 1 –.

Primary, secondary, and tertiary dressings used in the experiment. In the full thickness wounds, the meshed split thickness skin grafts were applied to the wound bed and were sprayed with ASCS. Half of the wounds were treated with control dressing as the primary dressings (A, left), while half of the wounds were treated with polymer as the primary dressing (A, right). Both primary dressings were covered in xeroform as the secondary dressing (B). A tie-over bolster was constructed as the outer dressing.

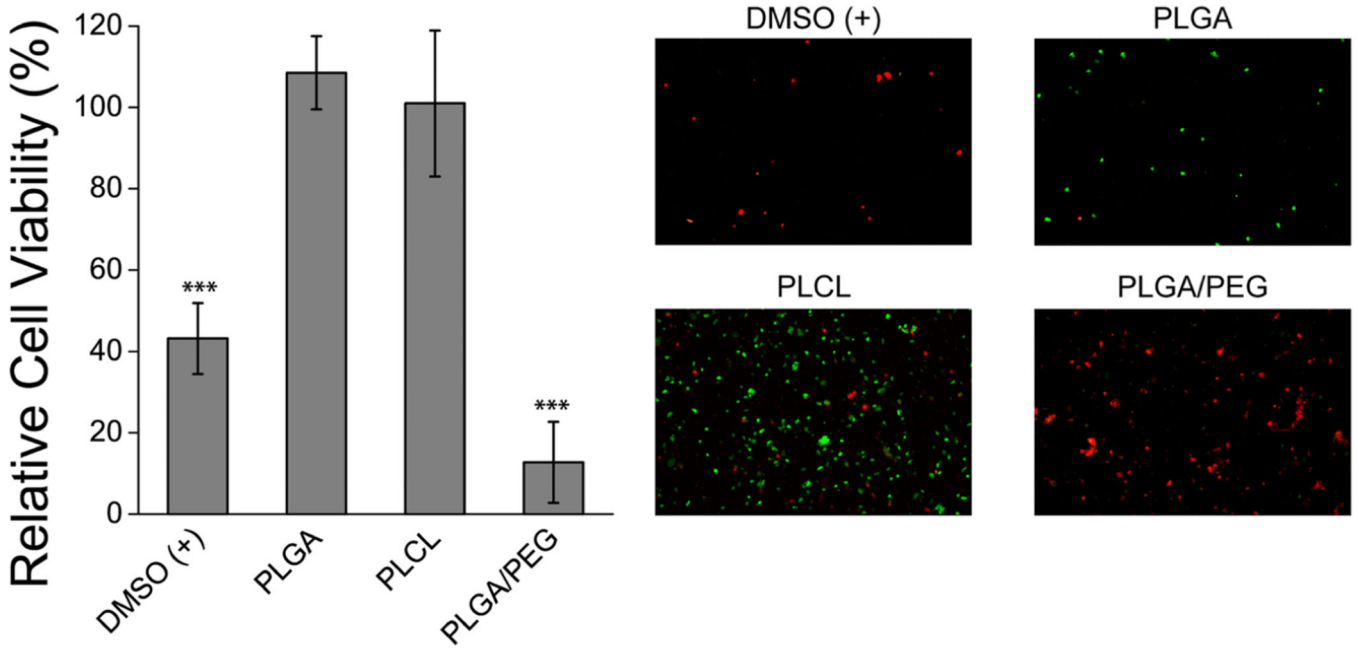

Fig. 2 –.

The PLGA and PLCL had no effect on ASCS relative cell viability. The ASCS viability was assessed with fluorescent staining. ASCS were processed in the presence of polymer disks. DMSO was used as a positive control. The green cells are live, red cells are dead. * **p < 0.001. (For interpretation of the references to colour in this figure legend, the reader is referred to the web version of this article.)

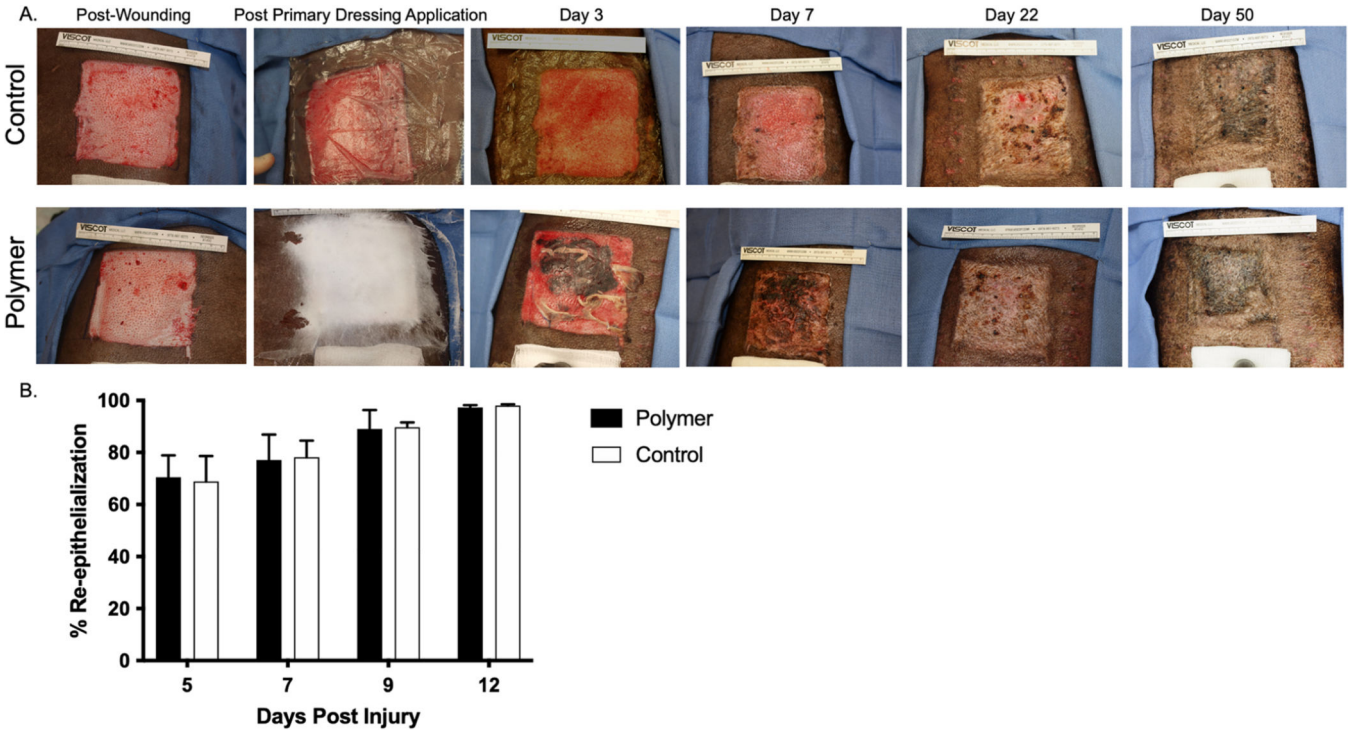

Fig. 3 –.

In Animal 1 in the most cranial wounds, DPTs treated with control or polymer healed in a similar manner. Re-epithelialization in DPT wounds was not altered by primary dressing treatment. Digital pictures (A) were taken at each time point after wounding, after primary dressing application, and on Days 3, 7, 22, and 50. Percent re-epithelialization (B) was measured from digital pictures in Image J at days 5, 7, 9, and 12 after injury.

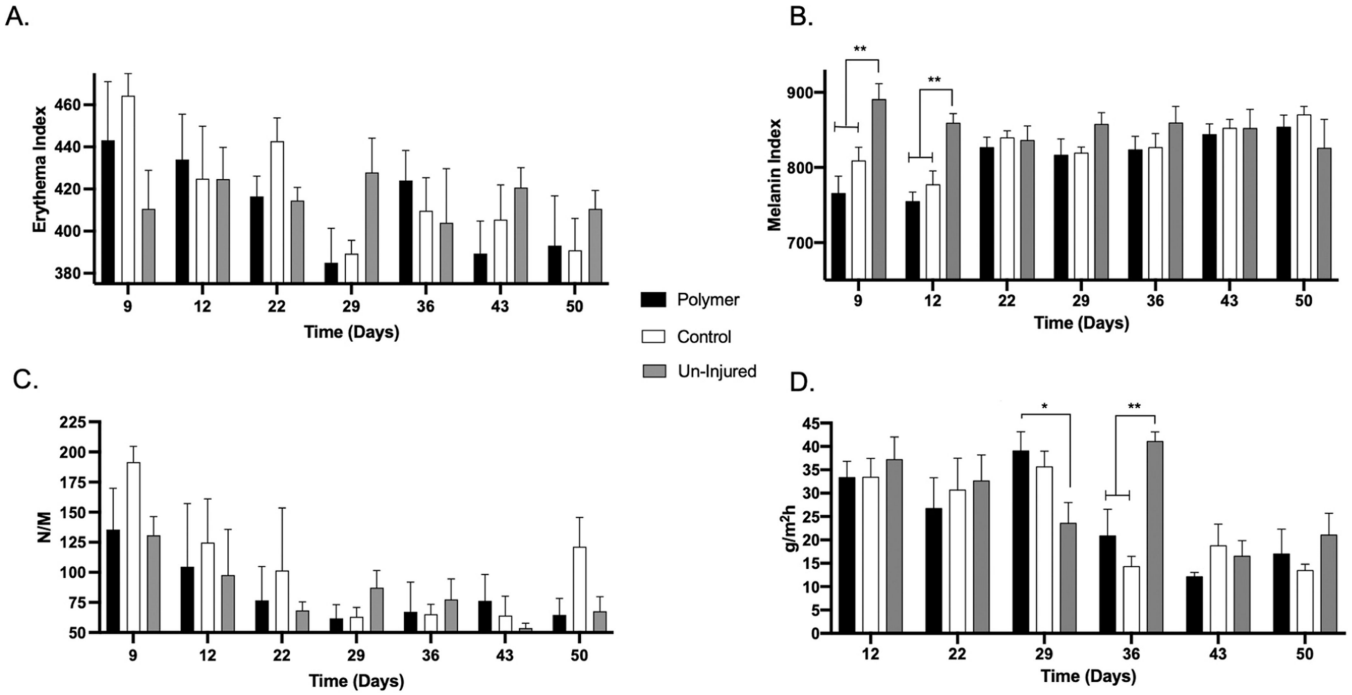

Fig. 4 –.

Erythema, melanin, elasticity, and TEWL in DPT wounds were not altered by primary dressing treatment. Erythema (A), melanin (B), elasticity (C), and TEWL (D) measured with non-invasive skin probes at days 5, 7, 9, 12, 22, 29, 36, 43, and 50 after injury, *$p < 0.05$, **$p < 0.01$.

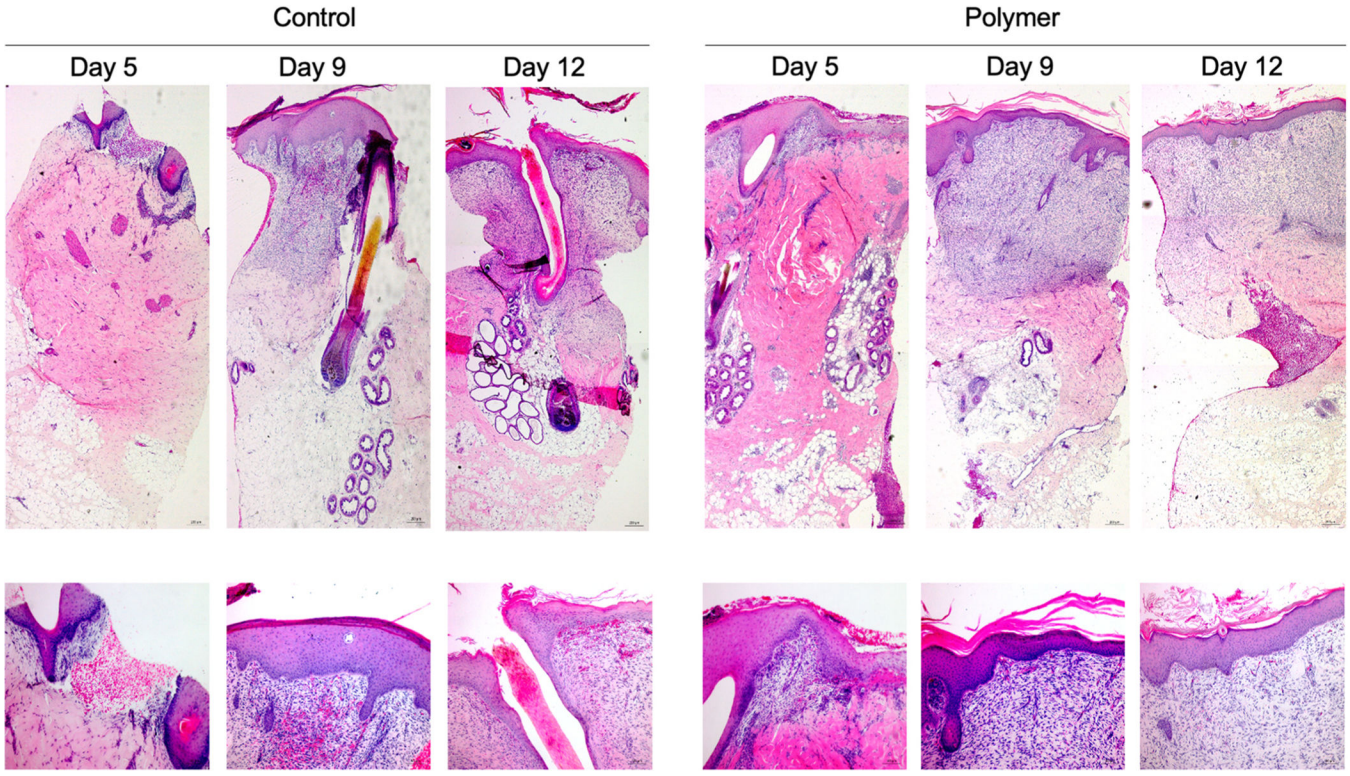

Fig. 5 –.

In Animal 1 in the most cranial wounds, H&E staining revealed similar histo-architecture between control vs. polymer groups in DPT wounds. Biopsies were taken at Days 5, 9, and 12 and were formalin fixed and paraffin embedded. Sections were then stained for H&E and images were captured for the control group (A) and polymer (B) at 5X magnification (top) and 10X magnification (bottom).

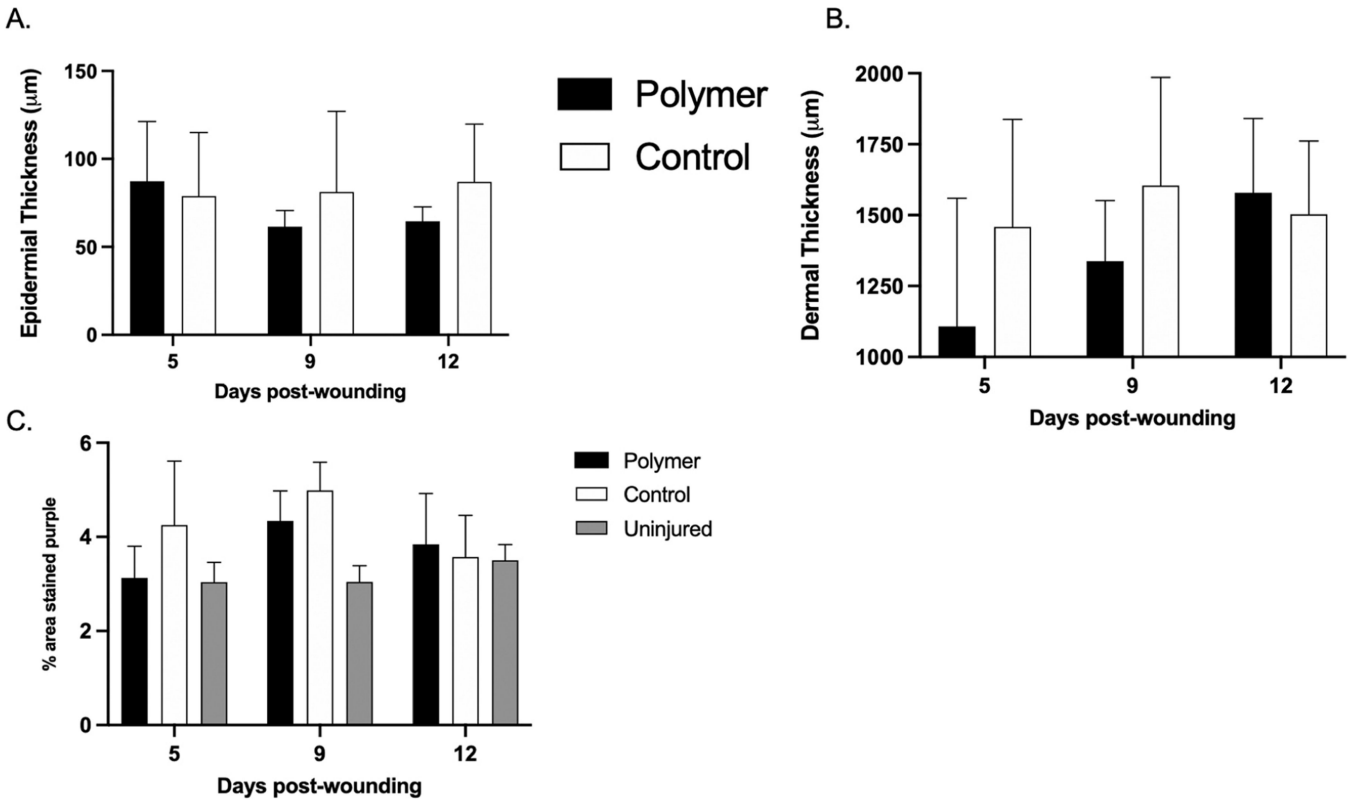

Fig. 6 –.

Epidermal and dermal thickness in DPT wounds were not altered by primary dressing treatment. Dermal cellularity in DPT wounds was not altered by primary dressing treatment. Biopsies were taken at Days 5, 9, and 12 and were formalin fixed and paraffin embedded. Sections were then stained for H&E and images were captured for the control and polymer groups. Epidermal (A), dermal thickness (B), and cellularity (C) were measured from these images using ImageJ software.

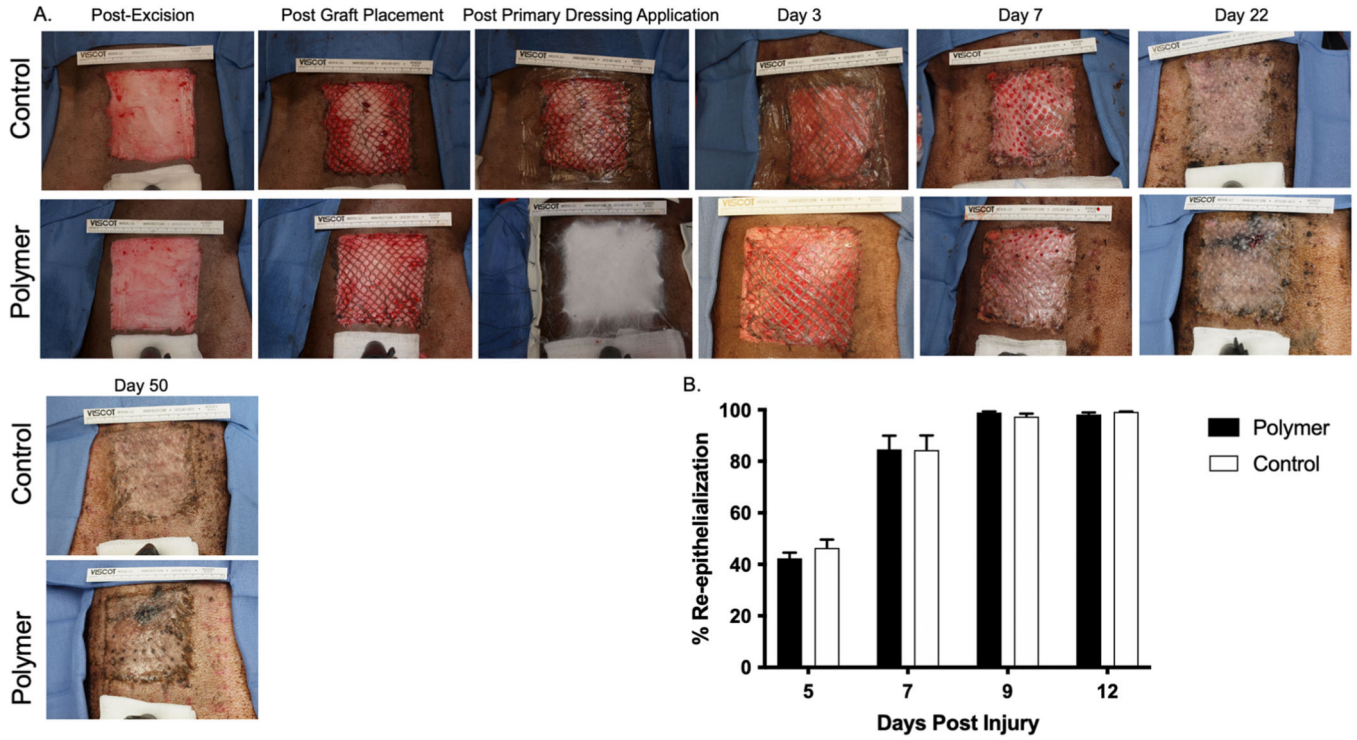

Fig. 7 –.

In Animal 3 in the most cranial wounds, FTs treated with control or polymer dressing healed in a similar manner. Re-epithelialization in FT wounds was not altered by primary dressing treatment. Digital pictures (A) were taken at each time point after wounding, after primary dressing application, and on Days 3, 7, 22, and 50. Percent re-epithelialization was measured from digital pictures in Image J at days 5, 7, 9, and 12 after injury (B).

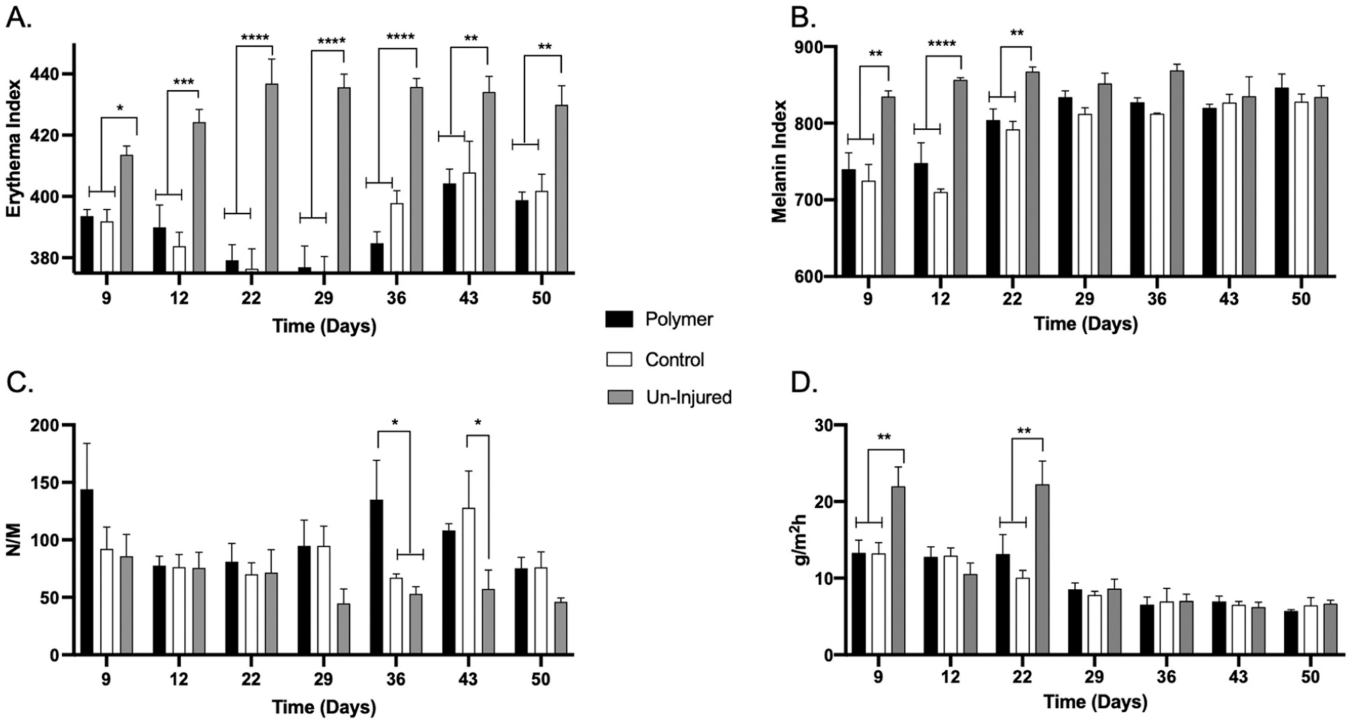

Fig. 8 –.

Erythema, melanin, elasticity, and TEWL in FT wounds were not altered by primary dressing treatment. Erythema (A), melanin (B), elasticity (C), and TEWL (D) measured with non-invasive skin probes at days 5, 7, 9, 12, 22, 29, 36, 43, and 50 after injury. *p < 0.05, * *p < 0.01, * **p < 0.001, * ** *p < 0.0001.

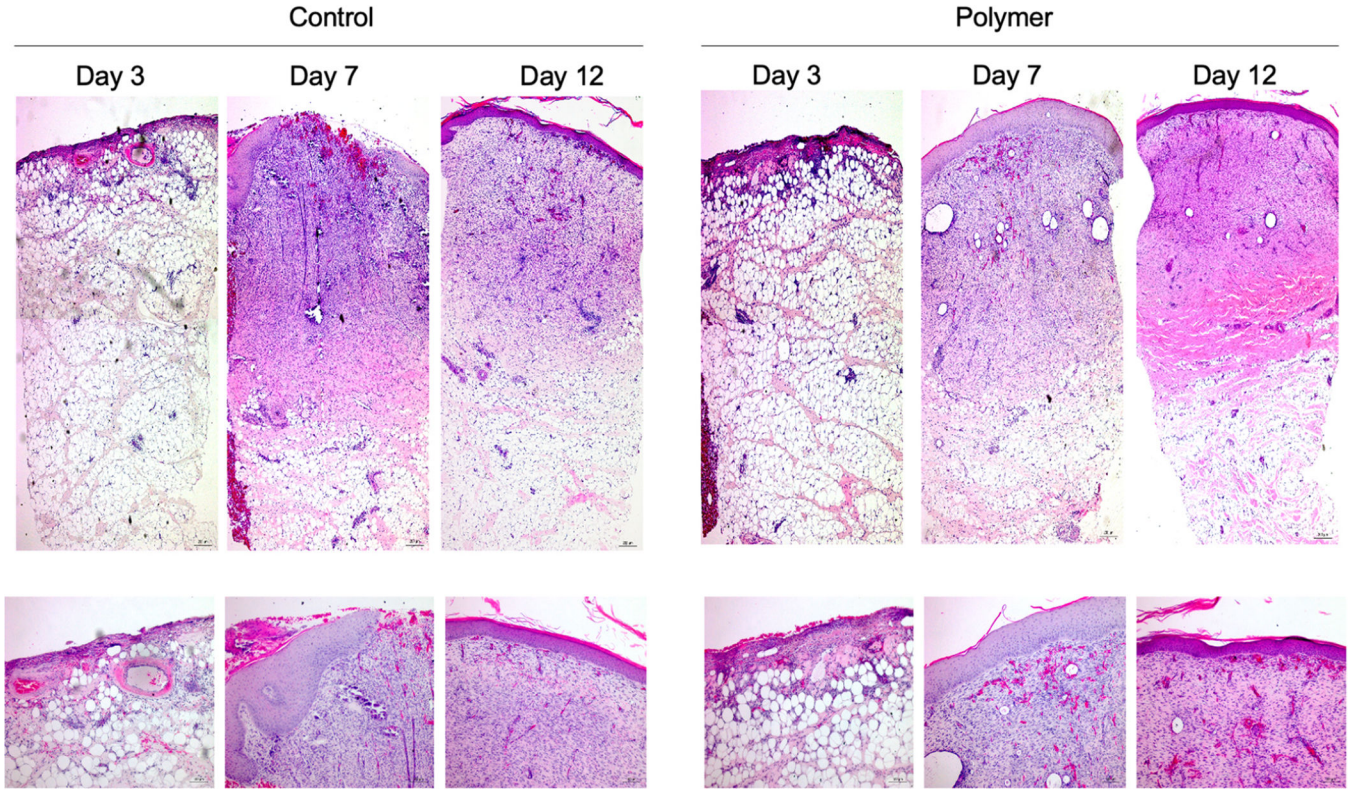

Fig. 9 –.

In Animal 3 in the most cranial wounds, H&E staining revealed similar histo-architecture between control vs. polymer groups in FT wounds in the biopsies taken from interstices. Biopsies were taken at Days 3, 7, and 12 and were formalin fixed and paraffin embedded. Sections were then stained for H&E and images were captured for the control group (A) and polymer (B) at 5X magnification (top) and 10X magnification (bottom).

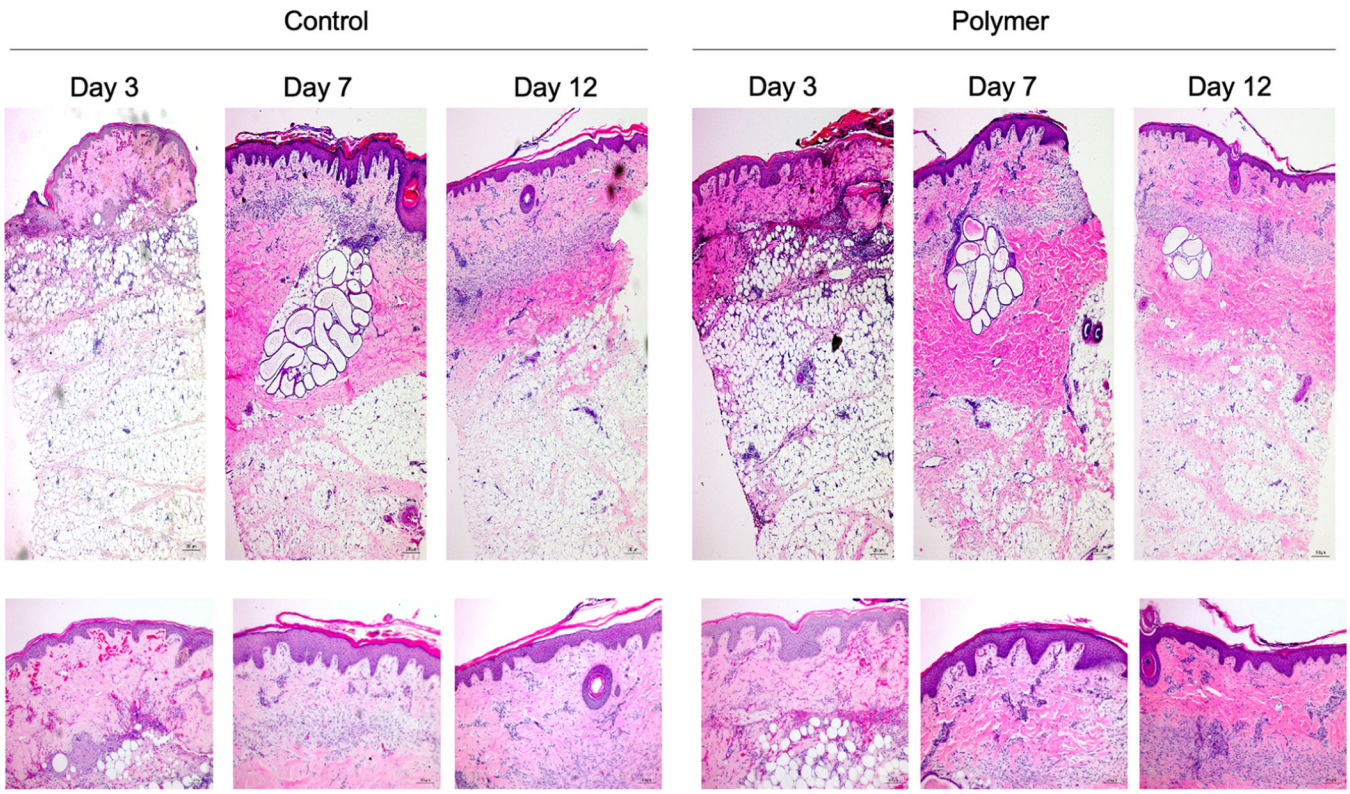

Fig. 10 –.

In Animal 3 in the most cranial wounds, H&E staining revealed similar histo-architecture between control vs. polymer groups in FT wounds in the biopsies taken from mSTSG. Biopsies were taken at Days 3, 7, and 12 and were formalin fixed and paraffin embedded. Sections were then stained for H&E and images were captured for the control group (A) and polymer (B) at 5X magnification (top) and 10X magnification (bottom).

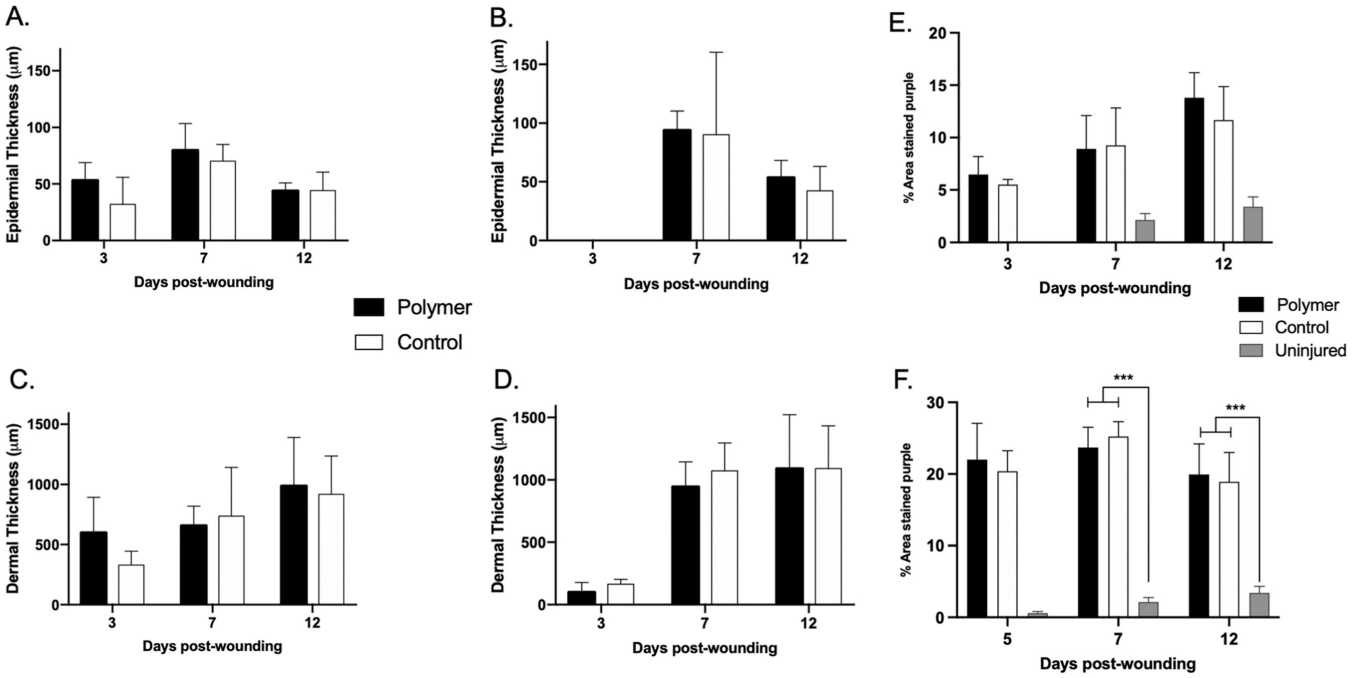

Fig. 11 –.

Epidermal and dermal thickness in FT wounds were not altered by primary dressing treatment. Dermal cellularity in FT wounds was not altered by primary dressing treatment. Dermal cellularity in FT wounds was not altered by primary dressing treatment. Biopsies were taken at Days 3, 5, 7, and 12 and were formalin fixed and paraffin embedded. Sections were then stained for H&E and images were captured for the control and polymer groups. Biopsies from mSTSGs (A, B and C) and interstices (D, E and F) were measured from these images using ImageJ software. * *$p < 0.01$, * **$p < 0.001$.

Table 1 –

Graft-loss in FT wounds treated with mSTSG and ASCS at Day 5.

Animal	Wound	Treatment	Grade
3	Right (cranial)	Polymer	0
	Right (caudal)	Control	2
	Left (cranial)	Control	1
	Left (caudal)	Polymer	1
4	Right (cranial)	Control	2
	Right (caudal)	Polymer	2
	Left (cranial)	Polymer	1.5
	Left (caudal)	Control	0.5